

# Synthesis and Spectroscopic and Electrochemical Properties of an Axially Symmetric Fullerene–Porphyrin Dyad with a Rigid Pyrrolo[3,4-*c*]pyrrole Spacer

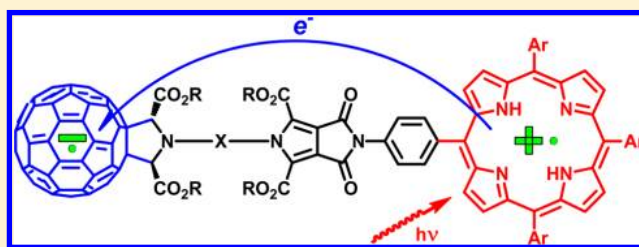
Alexander S. Konev,<sup>†</sup> Alexander F. Khlebnikov,<sup>\*,†</sup> Tamara G. Nikiforova,<sup>†</sup> Alexander A. Virtsev,<sup>†</sup> and Holm Frauendorf<sup>‡</sup>

<sup>†</sup>Department of Chemistry, Saint Petersburg State University, Universitetskii pr. 26, 198504 St. Petersburg, Russia

<sup>‡</sup>Institute of Organic and Biomolecular Chemistry, Georg-August-University, Tammannstrasse 2, D37077 Göttingen, Germany

## Supporting Information

**ABSTRACT:** A new approach to porphyrinofullerene donor–acceptor dyads, based on consecutive 1,3-dipolar cycloaddition of azomethine ylides, generated from bis-aziridinedicarboxylate, to C<sub>60</sub> and to porphyrin with a maleimidophenyl substituent, was developed. A synthesis of the axially symmetric porphyrin–fullerene–C<sub>60</sub> ensemble **5** with a novel rigid pyrrolo[3,4-*c*]pyrrolic linker was realized. Theoretical, electrochemical, and spectroscopic studies of compound **5** showed that it is capable of forming a charge-separated state.



## INTRODUCTION

Porphyrin–fullerene donor–acceptor dyads represent promising compounds for the creation of artificial photosynthetic systems due to their ability to form long-lived charge-separated (CS) states upon photoexcitation.<sup>1</sup> The long lifetime of the CS state is crucial for the following intermolecular electron transfer to occur.<sup>2</sup> The energy deposited in such a CS state can be further transformed either to electric power (solar cells) or to the energy of chemical bonds (catalysis). According to Marcus theory,<sup>3</sup> the following factors affect the lifetime of CS states at a given temperature: free Gibbs energy for charge recombination  $\Delta G_{\text{BET}}$  (BET, back-electron transfer), reorganization energy  $\lambda$ , and electronic coupling ( $V$ ) between donor and acceptor moieties (eq 1).

$$k_{\text{BET}} = [2\pi^{3/2}/(h(\lambda k_{\text{B}}T)^{1/2})]V^2 \exp(-(\Delta G_{\text{BET}} + \lambda)^2/(4\lambda k_{\text{B}}T)) \quad (1)$$

Porphyrin–fullerene dyads were reported to often possess small values of  $\lambda$  compared to  $\Delta G_{\text{BET}}$  ( $\lambda < -\Delta G_{\text{BET}}$ ). This moves the process of back-electron transfer into the Marcus inverted region, where the larger the driving force ( $\Delta G_{\text{BET}}$ ) the slower the process. That means that increasing  $\Delta G_{\text{BET}}$  would increase the efficiency of light energy conversion both by increasing the relative amount of transformed energy and by increasing the lifetime of the charge-separated state. Electronic coupling between donor and acceptor moieties depends on the length and nature of the bridge connecting the two fragments and on the topology and symmetry of the molecule. The dependence of the lifetime of the CS state on the distance between donor and acceptor fragments is not straightforward. On the one hand, a large separation distance between donor

and acceptor moieties benefits the prolongation of the CS state lifetime<sup>1</sup> by decreasing the electronic coupling between donor and acceptor. On the other hand, an increase in the distance between the reacting species increases the reorganization energy  $\lambda$  (eq 2), which has the opposite effect on the lifetime of the CS state<sup>1,3</sup>

$$\lambda = \lambda_{\text{out}} + \lambda_{\text{in}} \quad (2)$$

$$\lambda_{\text{out}} = e^2(4\pi\epsilon_0)^{-1}(d_{\text{donor}}^{-1} + d_{\text{acceptor}}^{-1} - R_{\text{center-to-center}}^{-1})(n^{-2} - \epsilon^{-1}) \quad (3)$$

where  $d_{\text{donor}}$ ,  $d_{\text{acceptor}}$ ,  $R_{\text{center-to-center}}$  are diameters of donor and acceptor counterparts and distance between their centers, respectively.

This is one of the reasons why the search for optimal geometry of molecular artificial photosynthetic systems is mostly a matter of trial and error.

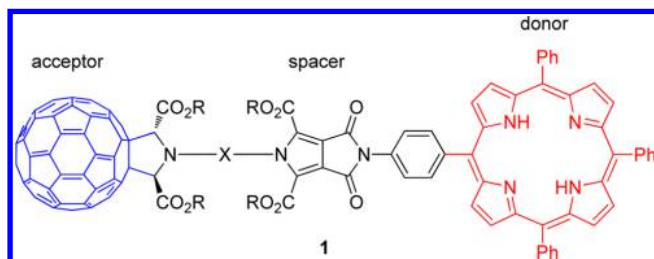
The synthesis and investigation of the photophysical properties of various porphyrin–fullerene covalent<sup>1,2,4,5</sup> and supramolecular donor–acceptor ensembles,<sup>2,6–9</sup> as well as ensembles of fullerene C<sub>60</sub> with other donors,<sup>10</sup> have already been performed. Different types of connection of the fullerene core to the rest of the molecule have been tried. Thus, the fullerene moiety was included in fullerene–porphyrin dyads as methanofullerene<sup>11–14</sup> aziridinofullerene,<sup>11</sup> Diels–Alder cycloadduct,<sup>15</sup> and pyrrolofullerene.<sup>11</sup> Various spacers have been used to connect fullerene with porphyrin fragments, both flexible and rigid. Among the first group are ethylene,<sup>12</sup> alkynyl

Received: December 20, 2012

and naphthyl glycols,<sup>11</sup> and silanes.<sup>16</sup> The second group includes steroids,<sup>11</sup> amides,<sup>17</sup> anthracene,<sup>15</sup> pyromellitimide,<sup>18</sup> rigid silanes,<sup>16</sup> and others.

Based on the bis-aziridine synthetic strategy recently suggested for the preparation of dumbbell-like bis- $C_{60}$ -fullerene triads,<sup>19</sup> we envisioned a novel type of spacer for porphyrin–fullerene donor–acceptor dyads, namely the pyrrolo[3,4-*c*]pyrrole system (Scheme 1). This spacer would provide (a)

Scheme 1



previously undescribed axial symmetry to the molecule, which can enhance electron-transfer, (b) rigidity of the molecule, fixing donor and acceptor at a certain and large distance preventing through space interaction and inhibiting back-electron transfer, and (c) facility to tune the electronic properties of the spacer and the solubility of the molecule by varying the bridge X and substituent R (Scheme 1).

## RESULTS AND DISCUSSION

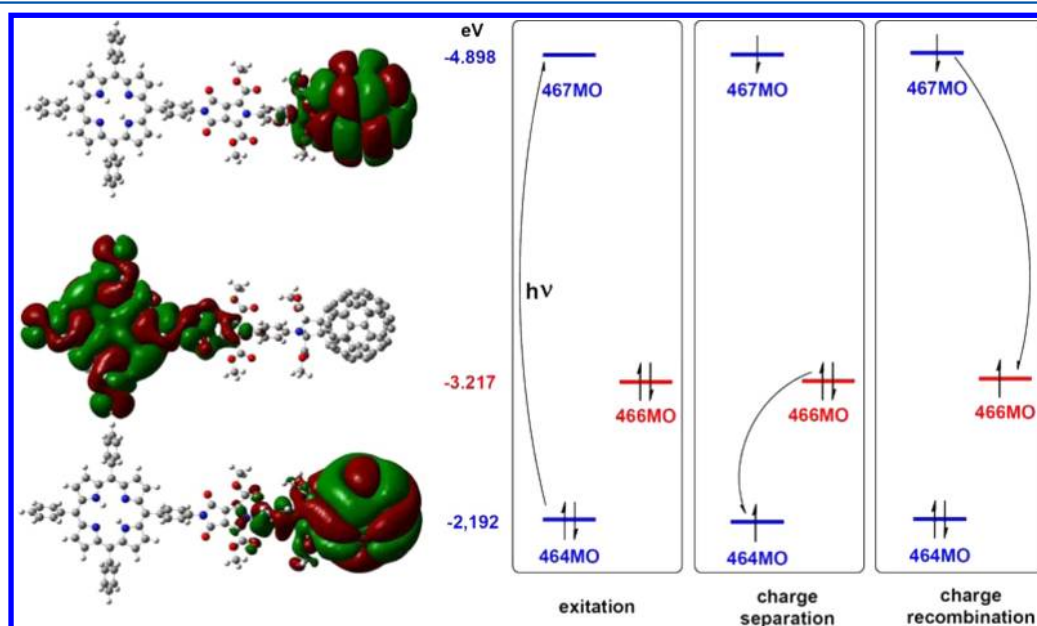
In order to estimate the ability of the porphyrin–fullerene dyad **1** to generate a long-lived CS state, we performed quantum chemical calculations on compound **2** (**1**, X = *p*-phenylene, R = Me) using DFT, the B3LYP functional, and the 6-31G(d) basis set. According to the calculations, the HOMO of molecule **2** is located mostly on the porphyrin moiety, while the LUMO is located on the fullerene cage (Figure 1). This is typical for fullerene–porphyrin dyads<sup>20</sup> and is the precondition for

generating a charge-separated state. The simple approach for the estimation of the ability of a molecule to form a long-lived CS state is based on the frontier molecular orbital description of photoinduced electron transfer.<sup>21</sup> Application of this approach to molecule **2** implies that the formation of the CS state proceeds via the local acceptor photoexcitation (transfer of an electron from 464MO to 467MO located on the fullerene moiety), followed by electron transfer involving orbital interactions between the HOMO localized on the donor (466MO) and a partly filled orbital of the acceptor (464MO). Charge recombination involves interactions between 467MO (LUMO) and 466MO (HOMO) (Figure 1). The overlap of the corresponding orbitals affects the value  $V$  in eq 1: the better the overlap, the higher is the rate of the corresponding process. As one can see from Figure 1, the overlap of 466MO and 464MO (corresponding to the formation of CS state) is significantly larger than the overlap of 467MO and 466MO (corresponding to charge-recombination), suggesting that  $V_{CS}$  will be larger than  $V_{BET}$ .

The values  $d_{donor} = 18.1$  Å,  $d_{acceptor} = 7.1$  Å,  $R_{center-to-center} = 25.0$  Å, taken from the optimized geometry of compound **2**, allows the estimation of the solvent reorganization energy  $\lambda_{out}$  from eq 3. The  $\lambda_{out}$  value strongly depends on the solvent used, e.g., for an unpolar solvent (benzene) it will be 0.007 eV, while for a polar solvent (1,2-dichloroethane) it will be around 0.9 eV. The internal reorganization energy  $\lambda_{in}$  is reported to range from 0.2 to 0.7 eV.<sup>21</sup> Hence, the total  $\lambda$  for compound **2** should range from 0.2 to 0.7 eV in a nonpolar solvent and from 1.1 to 1.6 eV in a polar solvent (Table 1).

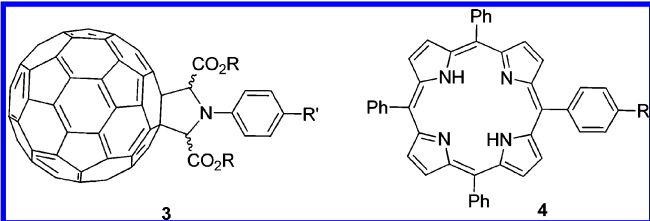
Table 1. Calculated Values of  $\lambda_{out}$  in Various Solvents

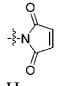
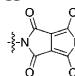
solvent	$n_D^{20}$	$\epsilon$	$\lambda_{out}$ , eV
benzene	1.5011	2.27	0.007
toluene	1.4969	2.38	0.058
dichloromethane	1.4241	8.93	0.857
<i>o</i> -dichlorobenzene	1.5514	9.93	0.708
1,2-dichloroethane	1.4448	10.36	0.861



**Figure 1.** FMO description of charge separation and charge recombination and visualization of MOs of molecule **2** (isovalue 0.001). MOs localized mostly on  $C_{60}$  are shown in blue, while MOs localized mostly on porphyrin fragment are shown in red.

Table 2. Experimental Data on  $E_{\text{red}}^{1/2}$  for Pyrrolofullerenes **3** and  $E_{\text{red}}^{1/2}$ ,  $E_{\text{ox}}^{1/2}$  for Porphyrins **4**, and FMO Energy Calculated in the Gas Phase at the B3LYP/6-31G(d) Level



Compound	R, R'	$E_{\text{red}}^{1/2}$ , V, vs. Ag/AgCl	$E_{\text{red}}^{1/2}$ , V, vs. Fc/Fc <sup>+</sup>	$E_{\text{ox}}^{1/2}$ , V, vs. Ag/AgCl	$E_{\text{LUMO}}$ , eV	$E_{\text{HOMO}}$ , eV
<i>trans</i> - <b>3a</b>	Et, MeO	−0.63	−1.10		−3.11	
<i>trans</i> - <b>3b</b>	Et, Me	−0.61	−1.08		−3.13	
<i>cis</i> - <b>3b</b>	Et, Me	−0.61	−1.08		−3.10	
<i>trans</i> - <b>3c</b>	Et, CN	−0.52	−0.99		−3.31	
<i>trans</i> - <b>3d</b>	Oct, MeO	−0.60	−1.08		−3.09	
<b>4a</b>		−0.58	−1.06	1.04	−2.77	−4.92
<b>4b</b>	H	−1.29	−1.77	1.03	−2.20	−4.91
<b>4c</b>		−1.29	−1.77	1.00	−2.17	−4.88

Another premise for the formation of a long-lived CS state is that the back-electron transfer (BET) process takes place in the inverted Marcus parabola region; i.e.,  $\lambda$  should be less than  $-\Delta G_{\text{BET}}$  ( $= -\Delta G_{\text{CR}}$ ). The latter value can be determined from eq 4.<sup>15</sup>

$$-\Delta G_{\text{CR}} = E_{\text{ox}} - E_{\text{red}} \quad (4)$$

The electrochemical oxidation and reduction potentials can be estimated from the HOMO and LUMO energy levels of the molecule, respectively, as it is known that a correlation exists between these two pairs of values.<sup>22–27</sup> However, as different equations have been reported for such a correlation, we synthesized, performed quantum-chemical calculations,<sup>29</sup> and measured electrochemical properties of a model series of pyrrolofullerenes **3**<sup>28</sup> and porphyrins **4** (Table 2) to find the corresponding correlations. For the purpose of better comparability of the results, the electrochemical potentials are also reported vs Fc/Fc<sup>+</sup> potential used as the external standard ( $E_{\text{red}}^{1/2}$  for Fc/Fc<sup>+</sup> relative to Ag/AgCl was 0.475 mV, see the Supporting Information). Least-squares approximation of the resulting trend gives eq 5 for the correlation between calculated MO energy level and experimental reduction or oxidation potential with  $R^2$  having a value of 0.99.<sup>29</sup>

$$E_{\text{red}}^{1/2} = -0.85E_{\text{LUMO(HOMO)}} - 3.19 \quad (5)$$

Use of eqs 4 and 5 allows the estimation of the free energy of charge recombination for compound **2** to be ca. −1.4 eV, which means that in nonpolar solvents the BET process will proceed in the inverted Marcus region ( $0.7 < 1.4$ ). Estimation of  $\Delta G_{\text{CS}}$  is possible from eq 6.<sup>15</sup>

$$-\Delta G_{\text{CS}} = E_{0-0} - (-\Delta G_{\text{CR}}) \quad (6)$$

As only a minor interaction in the ground state between donor and acceptor parts of the molecule is reported for systems similar to **2**,<sup>18</sup>  $E_{0-0}$  can be taken from the absorption spectrum of tetraphenylporphyrin **4b**. This gives the value of −0.5 eV for  $\Delta G_{\text{CS}}$ , suggesting that the forward electron transfer process might proceed in the inverted ( $\lambda = 0.2\text{--}0.7 \sim -\Delta G_{\text{ET}}$

$= 0.5$ ) Marcus parabola region, in almost optimal conditions ( $\lambda \sim \Delta G_{\text{ET}}$ ). It should also be noted that as  $\Delta G_{\text{CS}}$  has a negative value, the charge separation process can occur spontaneously from the thermodynamic point of view. Thus, the above theoretical results indicate that the rate of generation of the CS state in porphyrinofullerene **2** will be significantly larger than the rate of its decomposition via charge recombination, implying high probability of the formation of a long-lived CS state. This motivated us to elaborate the synthesis of the first compound of type **1** and investigate its spectral and electrochemical properties.

Retrosynthetic analysis of the target molecule **5** (Scheme 2), based on the bis-aziridine synthetic strategy,<sup>19</sup> leads to fullerene C<sub>60</sub>, bis-aziridine **6**,<sup>19</sup> and porphyrin **4a**.

Unsymmetrical *meso*-tetraarylporphyrins of A<sub>3</sub>B type, which porphyrin **4a** belongs to, could be obtained by stochastic

## Scheme 2

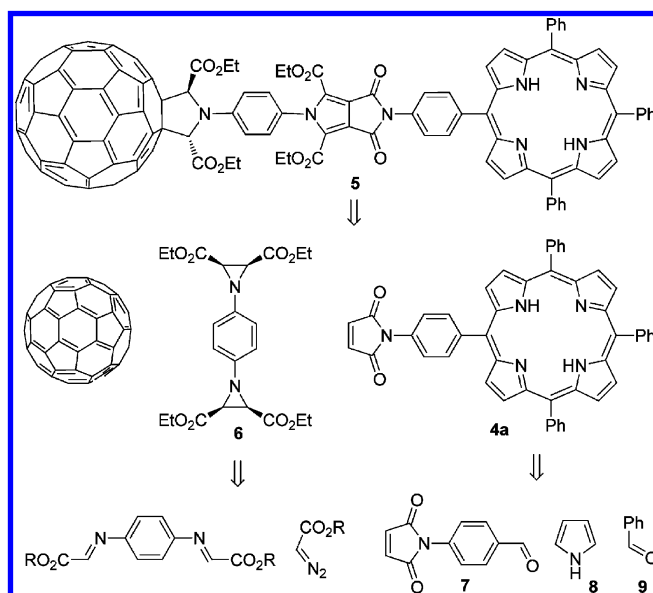
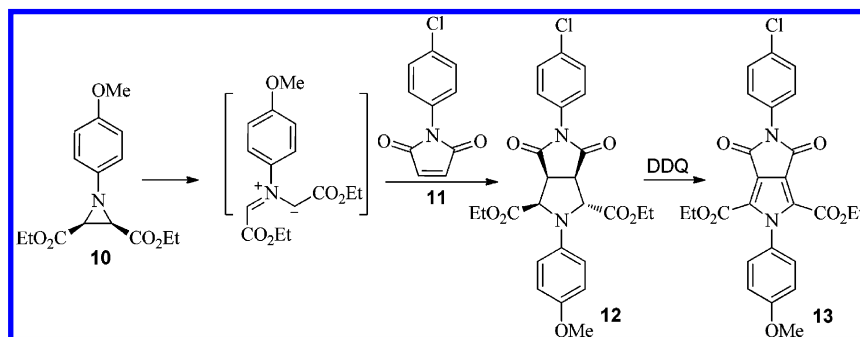


Table 3. Optimization of the Reaction Conditions for the Synthesis of Porphyrin 4a

$7 + 8 + 9 \xrightarrow[2) \text{ Oxidant}]{1) \text{ Catalyst}} 4a + 4b$						yield, %	
entry	catalyst	oxidant	conc of pyrrole, mol/L	heating mode <sup>a</sup>	time <sup>a</sup>	4a	4b
1	TfCl	air	10 <sup>-2</sup>	(1) rt (2) 40 °C	(1) 1 h (2) 4 h	3	13
2	TfCl	air	10 <sup>-2</sup>	(1) rt (2) 40 °C	(1) 1 h (2) 16 h	6	10
3	TfCl	MnO <sub>2</sub>	10 <sup>-2</sup>	(1) rt (2) rt	(1) 1 h (2) 20 h	5	2
4	TfCl	chloranil	10 <sup>-2</sup>	(1) rt (2) rt	(1) 1 h (2) 15 min	12	5
5	I <sub>2</sub>	DDQ	10 <sup>-1</sup>	(1) $\mu$ w 100 W/30 °C (2) $\mu$ w 100 W/30 °C	(1) 45 min (2) 25 min	6	17
6	I <sub>2</sub>	chloranil	10 <sup>-1</sup>	(1) $\mu$ w 100 W/30 °C (2) $\mu$ w 100 W/30 °C	(1) 45 min (2) 25 min	0.6	trace
7	I <sub>2</sub>	chloranil	1.3 × 10 <sup>-2</sup>	(1) $\mu$ w 100 W/30 °C (2) $\mu$ w 100 W/30 °C	(1) 40 min (2) 15 min	10	12
8	I <sub>2</sub>	chloranil	1.3 × 10 <sup>-2</sup>	(1) $\mu$ w 100 W/30 °C (2) $\mu$ w 100 W/30 °C	(1) 40 min (2) 1 min	2–17	11
9	I <sub>2</sub>	chloranil	1.3 × 10 <sup>-2</sup>	(1) $\mu$ w 100 W/30 °C (2) $\mu$ w 100 W/40 °C	(1) 40 min (2) 1 min	2–18	1–15
10	I <sub>2</sub>	chloranil	1.3 × 10 <sup>-2</sup>	(1) $\mu$ w 100 W/30 °C (2) $\mu$ w 100 W/40 °C	(1) 40 min (2) 5 min	2	trace
11	I <sub>2</sub>	chloranil	10 <sup>-2</sup>	(1) 30–32 °C (2) 30–32 °C	(1) 1 h (2) 10 min	13–16	7–10
12	I <sub>2</sub>	chloranil	10 <sup>-2</sup>	(1) 30–32 °C (2) 30–32 °C	(1) 1.5 h (2) 10 min	12	8
13	I <sub>2</sub>	chloranil	10 <sup>-2</sup>	(1) 30–32 °C (2) 30–32 °C	(1) 2 h (2) 10 min	12	8

<sup>a</sup>(1) Condensation. (2) Oxidation.

## Scheme 3



synthesis involving the Lewis acid catalyzed condensation of 4 mol of pyrrole, 3 mol of aldehyde A, and 1 mol of aldehyde B, followed by oxidation of the resulting porphyrinogen.<sup>30</sup> *N*-(4-Formylphenyl)maleimide 7, necessary for the synthesis of 4a, was prepared according to a published procedure.<sup>31</sup>

A literature survey shows that reactions catalyzed by molecular iodine<sup>30</sup> and triflyl chloride<sup>32</sup> give better yields of *meso*-tetraarylporphyrins than those catalyzed by other known catalysts such as BF<sub>3</sub>–etherate,<sup>33</sup> TFA,<sup>33</sup> PCl<sub>5</sub>,<sup>34</sup> propionic acid,<sup>35</sup> silica sulfuric acid/ZnCl<sub>2</sub>,<sup>36</sup> benzoic acids,<sup>37</sup> and cellulose sulfuric acid.<sup>38</sup> Therefore, the first two catalysts were tried for the synthesis of porphyrin 4a. According to literature, oxidation of the intermediate porphyrinogen can be performed by DDQ,<sup>33</sup> chloranil,<sup>39</sup> molecular oxygen,<sup>35</sup> and SeO<sub>2</sub>.<sup>40</sup> We have tried the first three oxidants. The results of the use of

various reaction conditions are summarized in Table 3. The best result was obtained by I<sub>2</sub>-mediated condensation followed by oxidation with chloranil (entry 11). In this case, porphyrin 4a was obtained in 13–16% yield along with 7–10% of *meso*-tetraphenylporphyrin 4b as a byproduct. Conducting the reaction under microwave irradiation gave an even higher yield of the target porphyrin of up to 18%. However, these experiments (entries 5–10) suffered from poor reproducibility, giving under the same conditions yields of porphyrin 4a from 2 to 18% (entry 9). When the reaction was performed under conventional heating, 2 h was required to consume all benzaldehyde. However, the maximum yield of porphyrin 4a was observed 1 h after the addition of the iodine, which is in accordance with the report of Lindsey.<sup>33</sup>



The use of the conditions originally reported for the  $\text{TfCl}$ -catalyzed synthesis of tetraaryl-substituted porphyrins (1 h at room temperature under an inert atmosphere followed by oxidation by air in boiling dichloromethane for 4 h, entry 1) gave a poor yield (3%) in our case. By increasing the time of the oxidation to 16 h (entry 2) it was possible to double the yield, indicating that oxygen is a very slow oxidant for this system. A comparable result was obtained using manganese dioxide as the oxidant (5% yield, entry 3), suggesting that heterogeneous oxidation does not proceed well for this reaction. Indeed, the use of a homogeneous oxidation with chloranil improved this result and porphyrin **4a** was obtained in 12% yield (entry 4). Thus, application of triflyl chloride gives no advantage over iodine in our case while requiring use of a more expensive reagent and a more complicated experimental technique. All the newly obtained compounds were fully characterized using standard spectral and analytical methods.

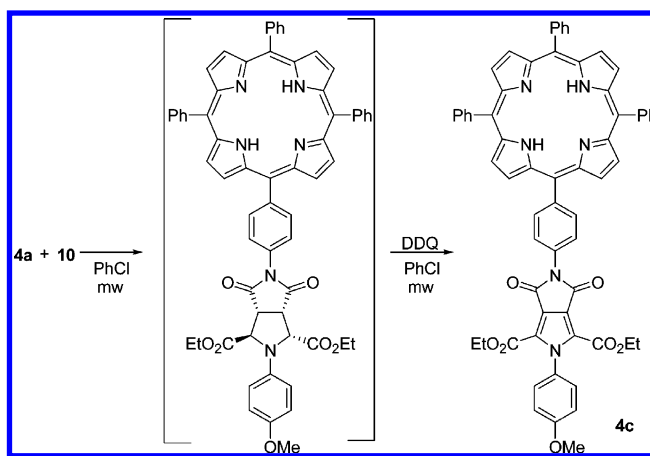
The key step of the synthesis of compound **5** involves a 1,3-dipolar cycloaddition of the azomethine ylide generated from the corresponding aziridine followed by aromatization of the resulting cycloadduct. To find optimal conditions for cycloaddition of azomethine ylides from aziridine dicarboxylates to maleimides the procedure was tested by reacting aziridine **10** and maleimide **11** (Scheme 3). Refluxing the mixture of these compounds in toluene or chlorobenzene for 32 h gave cycloadduct **12** in 65% yield. As microwave irradiation is known to often improve both the reaction time and yields,<sup>41–44</sup> we attempted to perform this reaction under microwave irradiation instead of conventional heating. Indeed, the reaction was complete after irradiation of a chlorobenzene solution of compounds **10** and **11** for 45 min (160 W, maximum temperature reached: 126 °C) to give cycloadduct **12** in 95%. The stereochemistry of cycloadduct **12** was confirmed by the observance of four signals (3.66, 4.01, 4.93, and 5.11 ppm) for the pyrrolidine protons in the  $^1\text{H}$  NMR spectrum, meaning that it has  $C_1$  symmetry and this is only possible if the relative configurations of the stereocenters in the 2,4- and 3,5-positions of the pyrrolidine ring are different. In addition, chemical shifts and spin–spin coupling constants in compound **13** are very close to those in similar compounds of known configuration.<sup>45</sup>

A number of reagents have been tested under various conditions to find the optimal way for aromatization of cycloadduct **12** to pyrrole **13**. The reaction did not proceed with sulfur as oxidant under conventional heating or microwave irradiation. Heating with palladium on carbon or chloranil resulted in formation of the desired product only in trace amounts. The use of  $\text{MnO}_2$  gave compound **13** only in 35% yield after heating in toluene under reflux for 32 h. Because of the heterogeneity of the reaction, a large excess of  $\text{MnO}_2$  (25 equiv) was required to achieve a satisfactory yield. Application of other solvents, such as benzene, DCM, or chlorobenzene gave no improvement. Finally, DDQ proved to be an excellent oxidant for the system under investigation. Thus, microwave irradiation of a chlorobenzene solution of cycloadduct **12** for 45 min gave the desired pyrrole **13** in 97% yield.

The procedure was tested on porphyrin **4a** using model aziridine **10**<sup>28</sup> as a reaction partner. Microwave irradiation of a solution of **4a** and **10** in chlorobenzene followed by immediate oxidation of the resulting adduct with DDQ gave porphyrin **4c** in 46% yield over two steps (Scheme 4).

The reaction of bis-aziridine **6** with fullerene  $\text{C}_{60}$  and porphyrin **4a** (Scheme 2) would lead to a complex mixture of products, as one can conclude from a study of the interaction of

Scheme 4



bis-aziridine **6** with fullerene  $\text{C}_{60}$ .<sup>19</sup> A more productive route to the target compound **5** (Scheme 5) involves cycloaddition of porphyrin **4a** and azomethine ylide from aziridine **14**, which can be synthesized by the reaction of fullerene  $\text{C}_{60}$  and bis-aziridine **6**.<sup>19</sup>

We found that the use of a 10-fold excess of porphyrin **4a** and relatively mild reaction conditions (heating in chlorobenzene at 90 °C) gives the maximum yield of the intermediate diastereomeric cycloadducts **15** (Table 4). In this case, the yield of the mixture of cycloadducts **15** comprised 80–85% as opposed to the value of ~50% typical for the experiments with the lesser ratio of aziridine: porphyrin (1:4 or 1:2) and/or higher temperatures (100 or 120 °C). The oxidation of the intermediate cycloadducts did not proceed at 100 °C or lower temperatures. The desired product is formed under oxidation only at 120 °C or higher in 5–13% yield based on starting aziridine. A significant improvement of this result was obtained by the use of microwave irradiation. In this case, when the reaction mixture was irradiated for 30 min (160 W, maximum temperature attained during the reaction was 127 °C) the yield of the target porphyrinofullerene **5** was 42%. Application of the microwave irradiation also for the first step and performing the reaction in a one-pot mode without isolation of the intermediate cycloadducts gave a poorer yield of 8.5%. Thus, the best conditions for the synthesis of the target porphyrinofullerene **5** are a result of performing the cycloaddition of aziridine **14** to porphyrin **4a** at 90 °C under conventional heating, followed by isolation of the cycloadducts **15** by flash chromatography and then oxidation of **15** with DDQ under microwave heating (160 W, 127 °C).

Ionization of **5** was achieved by ESI to give low-intensity molecular ion (calcd for  $\text{C}_{130}\text{H}_{56}\text{N}_7\text{O}_{10}^+$   $[\text{M} + \text{H}]^+$ , 1874.4083, found 1874.4064). Field desorption (FD) ionization was, therefore, applied for further mass spectrometric detection of this compound. Under the soft ionization conditions used for field desorption, the molecular ion was formed by removal of an electron under exposure to a high voltage (10 kV) without extensive fragmentation. The simulated isotopic pattern of the molecular ion of **5** fits perfectly the experimental one (Figure 2).

The  $^1\text{H}$  NMR spectrum of **5** contains signals for the porphyrin NH protons at –2.82 ppm. Pyrrole rings A show two doublets at 8.94 and 8.84 ppm ( $J = 4$  Hz). The latter is poorly resolved from the signals of pyrrole rings B, which shows a singlet at 8.83 ppm. The *ortho*-protons of phenyl groups appear

### Scheme 5

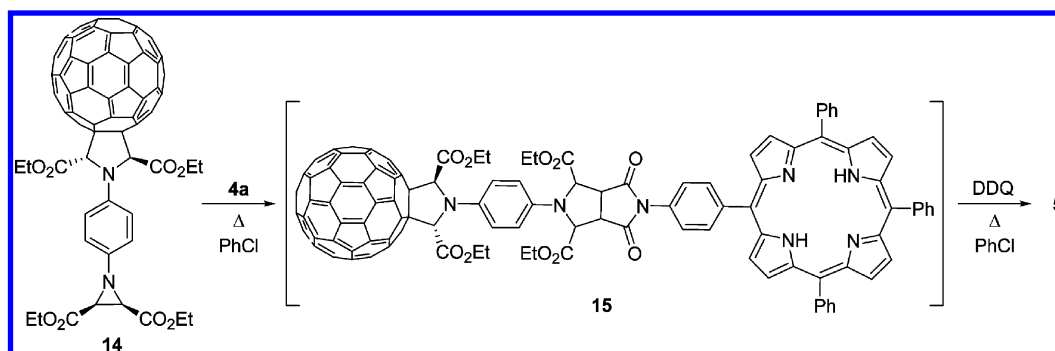
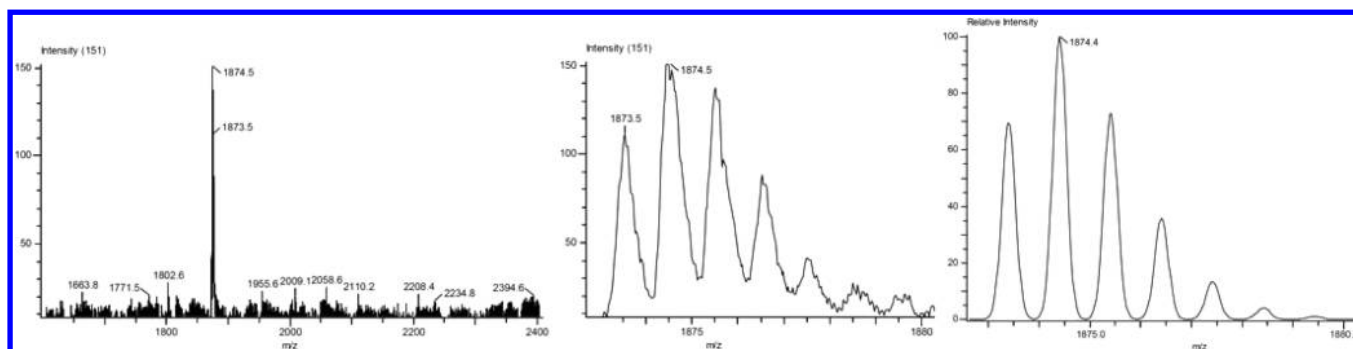


Table 4. Optimization of Reaction Conditions for the Synthesis of Porphyrinofullerene 5

entry	ratio 14:4a	heating mode <sup>a</sup>	time, <sup>a</sup> h	yield, %	
				15	5
1	1:4	(1) 100 °C	(1) 12	48	19
		(2) $\mu$ w 160 W/max temp 127 °C	(2) 1		
2	1:2	(1) 120 °C	(1) 3	48	0
		(2) 120 °C	(2) 9		
3	1:10	(1) 100 °C	(1) 12	20	5
		(2) $\mu$ w 160 W/max temp 127 °C	(2) 1		
4	1:10	(1) $\mu$ w 160 W/max temp 127 °C	(1) 0.5	without isolation	8.5
		(2) $\mu$ w 160 W/max temp 127 °C	(2) 1.5		
5	1:10	(1) 90 °C	(1) 24	84	13
		(2) 120 °C	(2) 6		
6	1:10	(1) 90 °C	(1) 22	79	42
		(2) $\mu$ w 160 W/max temp 127 °C	(2) 0.5		

<sup>a</sup>1) Condensation. (2) Oxidation.

**Figure 2.** FD-mass spectrum of porphyrinofullerene **5**; experimental (left) and simulated (right) isotopic pattern of the molecular ion of **5**.

as a multiplet at 8.15–8.25 ppm with an intensity of 6 protons, *meta*- and *para*-protons appear as a multiplet at 7.70–7.80 ppm with an intensity of 9 protons. The protons of the benzene ring adjacent to the porphyrin core appear as a doublet of doublets at 8.39 and 7.83 ppm ( $J = 8$  Hz). The protons of the benzene ring adjacent to the pyrrolidine unit appear as a doublet of doublets at 7.50 and 7.39 ppm ( $J = 8.5$  Hz). That these sets of doublets belong to the same AB systems is confirmed by the observance of the corresponding cross-peaks in COSY spectrum (see the Supporting Information). Two pyrrolidine protons of the pyrrolofullerene unit appear as a singlet at 6.49 ppm with an intensity of two protons. The value is characteristic for *trans*-pyrrolofullerenes of this kind.<sup>19,28</sup> Two sets of signals are observed for the two kinds of ethyl groups presented in the molecule. According to the COSY spectrum (see the Supporting Information), ethyl groups of one kind

appear as a quartet at 4.36 ppm and a triplet at 1.40 ppm ( $J = 7$  Hz), while the ethyl groups of another type appear as a multiplet at 4.25–4.32 and a triplet at 1.20 ppm ( $J = 7$  Hz).

The  $^{13}\text{C}$  NMR spectrum of **5** contains 57 signals (see the Supporting Information). There are six signals in the aliphatic region: two methyl groups at 14.4 and 14.5 ppm, two methylene groups at 62.30 and 62.32 ppm, newly formed  $\text{sp}^3$ -carbons of the fullerene cage at 71.2 ppm, and remaining pyrrolidine carbon at 74.9 ppm. The carbonyl groups give signals at 169.9 and 161.1 ppm. Though there are three kinds of carbonyl groups in the molecule, the observation of only two signals is most probably caused by the overlapping of two signals. Taking into account that for compound **4c** (same as for compound **4a**) three phenyl rings of the triphenylporphyrin fragment show four signals, and the porphyrin core shows up to six signals, one of which is a broad singlet at ca. 130 ppm, one

would expect for the *trans*-compound **5**, which has  $C_2$  symmetry, 49 signals in the aromatic region of the spectrum. That is in fact the case. If the pyrrolidine ring had *cis*-configuration, the molecule would have  $C_s$  symmetry, and therefore the number of signals in the aromatic region of the spectrum would be 51.

The electronic absorption spectra in the ultraviolet and visible range of porphyrinofullerene **5** and model compounds **4** are presented in Figure 3. The Soret band lies at 417–418 nm

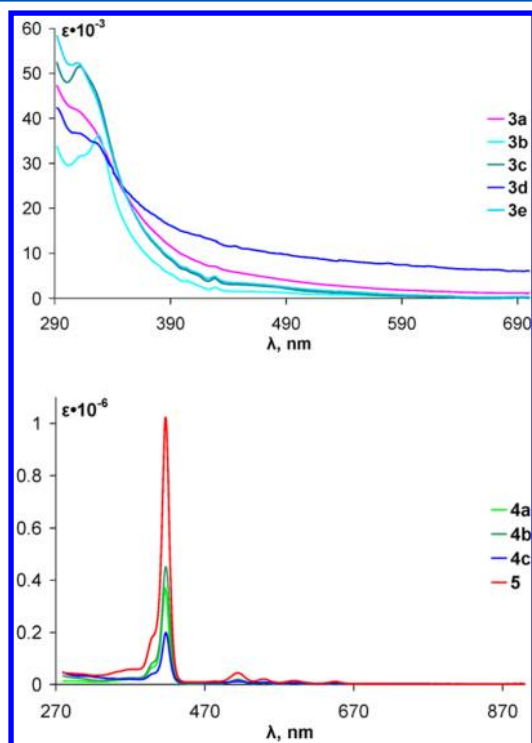


**Figure 3.** Electronic absorption spectra in  $\text{CH}_2\text{Cl}_2$  of pyrrolofullerenes **3**,  $c \approx 10^{-5} \text{ mol}\cdot\text{L}^{-1}$ , and porphyrins **4a–c**, **5**,  $c \approx 10^{-3} \text{ mol}\cdot\text{L}^{-1}$ .

for all four compounds, four Q-bands are observable at 514, 549, 589, and 645 nm. The absorption band of the fullerene cage can be observed for compound **5** at 310 nm with a shoulder at 325 nm. Analysis of the data obtained for a series of model pyrrolofullerenes **3** shows that a different pattern can be observed for these two bands. They can appear either as two distinct bands with maxima at 312 and 329 nm, with the band at longer wavelength being more intensive, or as a band at ca. 310 nm with a shoulder at ca. 325 nm (Figure 3), which confirms the assignment made. No interaction can be observed in the ground state between the donor (porphyrin) and acceptor (fullerene) moieties of compound **5**.

The fluorescence spectrum of compound **5** was recorded in  $\text{CHCl}_3$  with excitation at the wavelength of maximum absorption (419 nm) (Figure 4). It reveals an emission spectrum typical for tetraphenylporphyrin **4b** with two emission maxima at 653 and 720 nm, similar to that reported for **4b** (650 and 714 nm).<sup>46</sup> The quantum yield of fluorescence of **5** is diminished compared that of **4b** (0.07 vs 0.11<sup>47–51</sup>). The fluorescence quenching might be caused by a charge transfer process. The data obtained along with the literature reported fluorescence lifetime for **4b**<sup>52</sup> (9.16 ns,  $\text{CHCl}_3$ ) (9.32 ns, toluene)<sup>53</sup> made it possible to evaluate the upper bound of the

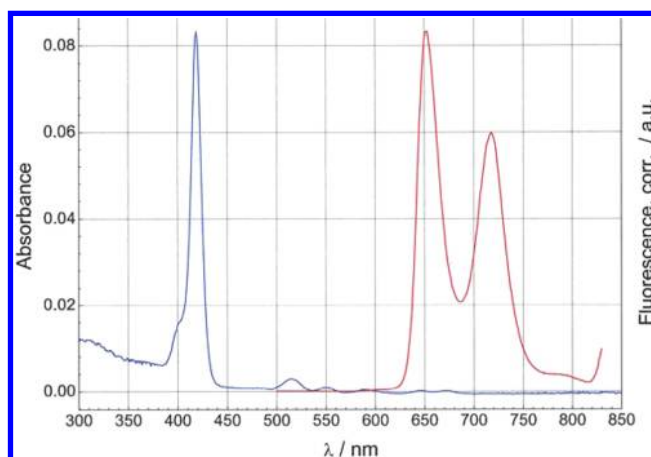


**Figure 4.** Fluorescence spectrum of compound **5** in  $\text{CHCl}_3$ .

rate constant for charge transfer in **5** to be  $6.2 \times 10^7 \text{ s}^{-1}$  (eq 7).<sup>21</sup>

$$k_{cs} = (\Phi_{(4b)}^F / \Phi_{(s)}^F - 1) / \tau_{(4b)}^F \quad (7)$$

## ELECTROCHEMISTRY

The electrochemical properties of porphyrinofullerene **5** were studied by cyclic voltammetry in a 0.1 M solution of tetra-*n*-butylammonium perchlorate  $[(\text{TBA})\text{ClO}_4]$  in *o*-dichlorobenzene (*o*-DCB). The CVA of **5** is characterized by three peaks in the region of negative potentials and one peak in the region of positive potentials (Figure 5). The presence of the same

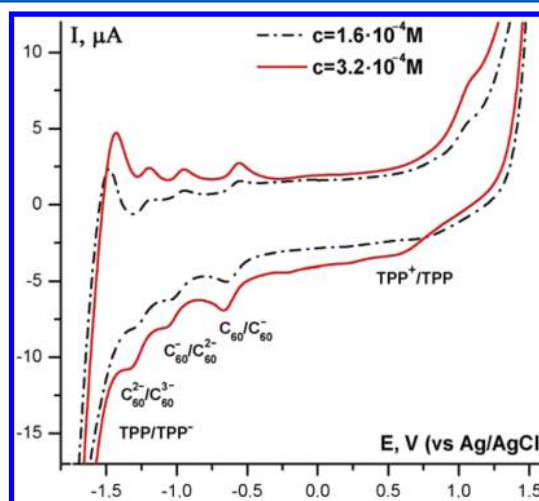


**Figure 5.** CVA curves of compound **5** (various concentrations) in a 0.1 M solution of  $(\text{TBA})\text{ClO}_4$  in *o*-DCB at scan rate 10 mV/s.

number of peaks both in cathodic and anodic waves and the proximity of their values indicate that they correspond to reversible redox processes. However, the observed dependence of peak potentials ( $E_p$ ) on the scan rate (Figure 6 and Table 5) means that the electrochemical processes proceed in a quasi-reversible way.

To assign the observed peaks, we have performed a CVA study of model compounds: tetraphenylporphyrin **4b**, porphyrin **4a**, pyrroloporphyrin **4c**, and pyrrolofullerenes **3**. The following conclusions have been made from this study: (1) The pyrrolo[3,4-*c*]pyrrole system is electrochemically inert in



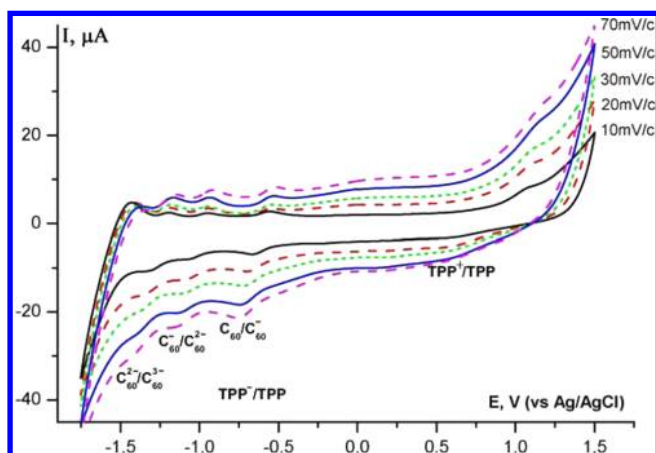


**Figure 6.** CVA curves of compound **5** ( $c = 3.2 \times 10^{-4}$  M) in a 0.1 M solution of (TBA)ClO<sub>4</sub> in *o*-DCB at various scan rates.

**Table 5.** Peak Potentials  $E_p$  (V) and Selected  $E_{red}^{1/2}$  (V) for Compound **5** at Various Scan Rates

scan rate, mV/s	$E_{p1}$	$E_{p2}$	$E_{p3}$	$E_{p4}$	$E_{red}^{1/2} 1$	$E_{red}^{1/2} 2$	$\Delta E_{red}^{1/2}$
10	0.59	-0.67	-1.07	-1.33	0.76	-0.59	1.34
20	0.56	-0.70	-1.09	-1.35	0.73	-0.61	1.34
30	0.58	-0.71	-1.10	-1.37	0.72	-0.62	1.34
50	0.55	-0.74	-1.13	-1.39	0.70	-0.65	1.35
70	0.56	-0.76	-1.15	-1.40	0.70	-0.66	1.36

the range of -1.75 to +1.5 V, since only the peaks of the porphyrin system are observed for pyrroloporphyrin **4c** at 0.93 and -1.40 V (Figure 7). (2) The maleimide moiety in

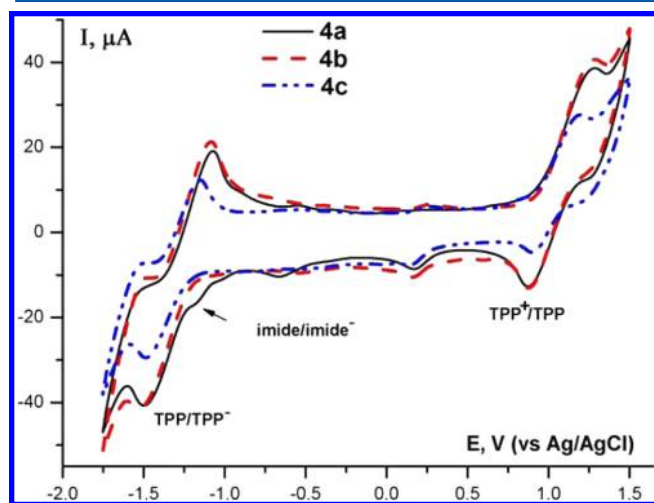


**Figure 7.** CVA curves of porphyrins **4a** ( $c = 2 \times 10^{-3}$  M), **4b** ( $c = 2 \times 10^{-3}$  M), and **4c** ( $c = 1.4 \times 10^{-3}$  M) in the same media, scan rate 10 mV/s.

porphyrin **4a** reveals some electrochemical activity as minor quasi-reversible peaks were observed at -0.64, -1.03, and -1.13 V (Figure 7). (3) Three quasi-reversible peaks are observed for pyrrolofullerenes **3** in the range -2 to 0 V (Figure 8). (4) The observed peaks for **5** in the negative potentials range correspond to the first three reductions of the fullerene cage and to the first reduction of the porphyrin system. The last peak overlaps with the peak for the third reduction of C<sub>60</sub>. The

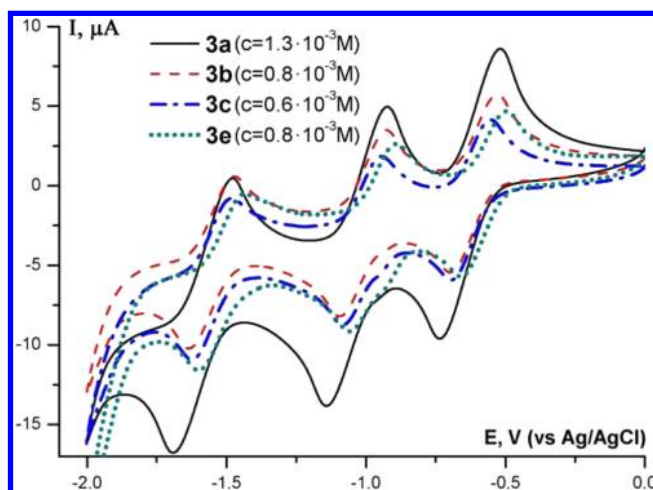


**Figure 8.** CVA curves of pyrrolofullerenes **3a–b** and **3e** ( $R = Et$ ,  $R' = I$ ) in the same media, scan rate 10 mV/s.

peak in the positive potentials range corresponds to the first oxidation of the porphyrin ring.

Positions of the fullerene peaks in compound **5** are almost the same as those in fulleropyrrolidines **3**, suggesting only a minor influence of the porphyrin fragments to the fullerene core in **5** (Table 6). Interestingly, the peak for oxidation of porphyrin is significantly shifted to zero potential, implying that the fullerene fragment facilitates oxidation of the porphyrin moiety in compound **5**.

The obtained experimental data (Table 6 and Figure 3) allow the  $\Delta G_{CR}$  and  $\Delta G_{CS}$  of porphyrinofullerene **5** to be calculated (eq 4 and 6,  $E_{0-0} = 1.92$  eV from the electron absorption spectrum of **5**) to obtain the values of -1.26 and -0.66 eV, respectively. These values of  $\Delta G_{CR}$  and  $\Delta G_{CS}$  are reasonably close to our preliminary estimates (vide supra).

## CONCLUSIONS

A novel synthetic approach toward porphyrinofullerene donor–acceptor dyads based on consecutive 1,3-dipolar cycloadditions of azomethine ylides, generated from bis-aziridine, to C<sub>60</sub> and then to porphyrin with a maleimidophenyl substituent was developed. The synthesis of a new axial symmetrical porphyrin–fullerene–C<sub>60</sub> dyad **5** with a novel rigid pyrrolo[3,4-*c*]pyrrolic linker was performed. Preliminary theoretical, electrochemical, and spectroscopic studies of compound **5** show that it is capable of forming a charge-separated state and therefore it might be interesting for solar cell application. Synthesis of further derivatives of **1** and determination of the lifetime of the charge-separated state for compound **5** is currently underway.

## EXPERIMENTAL SECTION

**General Methods.** Melting points were determined on a hot stage microscope and are uncorrected. IR spectra were recorded on FTIR Instrument. <sup>1</sup>H (300 or 600 MHz) and <sup>13</sup>C (75 or 125 MHz) NMR spectra were determined in CDCl<sub>3</sub>, C<sub>6</sub>D<sub>6</sub>, or (CD<sub>2</sub>Cl)<sub>2</sub>. Chemical shifts ( $\delta$ ) are reported in ppm downfield from tetramethylsilane. HRMS was performed using a 7T-FTICR mass spectrometer equipped with an electrospray ion source applying an electrospray voltage of 4.2 kV, microTOF mass spectrometer, and MS Q-TOF. Field desorption measurements were carried out on a TOF mass spectrometer using a FD emitter with an emitter voltage of 10 kV. The reactions under microwave irradiation were carried out in a sealed flask in a Minotavr-2 microwave oven for laboratory experiments. Flash



Table 6. Peak Potentials  $E_p$  (V) and  $E_{red}^{1/2}$  (V) for Compounds 3–5 and  $C_{60}$  (Scan Rate: 10 mV/s)

compd	$E_{p1}$	$E_{p2}$	$E_{p3}$	$E_{p4}$	$E_{red}^{1/2}{}_1$	$E_{red}^{1/2}{}_2$
5	0.59	−0.67	−1.07	−1.33	0.76	−0.59
4a	0.95	−0.64	−1.13	−1.38	1.04	−0.58
4b	0.94			−1.41	1.03	−1.29
4c	0.93			−1.40	1.00	−1.29
$C_{60}$		−0.72	−1.16	−1.64		−0.58
3a–e		−0.58 to −0.74	−1.03 to −1.18	−1.51 to −1.74		−0.52 to −0.63

chromatography was performed using silica (0.040–0.063 mm). TLC analysis was performed on glass backed plates coated with a 0.2 mm silica layer with UV-indicator 60F254. UV–visible absorption spectra were recorded on UV–vis spectrophotometer, and fluorescence spectra on a fluorescence spectrophotometer. Quantum chemical calculations were performed using a Gaussian 09 package.

**Electrochemistry.** The electrochemical measurements were carried out using an AUTOLAB12 PGSTAT12, connected through an interface with a PC. Cyclic voltammograms were recorded in a hermetically sealed three-electrode glass electrochemical cell. A platinum disk electrode ( $d = 6$  mm) was used as the working electrode. A platinum wire served as the counter electrode. An Ag/AgCl electrode was used as the reference electrode, tetra-*n*-butylammonium perchlorate (0.1 M) as supporting electrolyte and dry *o*-DCB as a solvent. All solutions were purged prior to electrochemical measurements using argon gas. CVA curves were recorded under an argon atmosphere at various potential sweep rates (10, 20, 30, 50, and 70 mV/s) for compounds 3a–e, 4a–c, and 5 (see the Supporting Information). In most cases, potentials are referenced to a Ag/AgCl electrode. Where ferrocene is specified as a reference, it was used as an external standard with the CVA experiment being conducted under the same conditions.

**N-(4-Formylphenyl)maleimide (7).** Synthetic procedure is reported elsewhere.<sup>31</sup> Light yellow crystals: mp 114–120 °C (lit.<sup>30</sup> 130–131 °C);  $^1H$  NMR ( $CDCl_3$ , 300 MHz)  $\delta$  6.93 s (2H), 7.65 pseudo d (2H,  $J = 8.43$  Hz), 8.01 pseudo d (2H,  $J = 8.43$  Hz), 10.06 s (1H);  $^{13}C$  NMR ( $CDCl_3$ , 75 MHz)  $\delta$  125.6, 130.4, 134.4, 134.8, 136.5, 168.7, 191.1.

**Porphyrin 4a.** A mixture of aldehyde 7 (50 mg, 0.25 mmol), benzaldehyde (80 mg, 0.75 mmol), and pyrrole (67 mg, 1 mmol) in dichloromethane (100 mL) was vigorously stirred while being heated to 28 °C during 3 min. Iodine (25 mg, 0.1 mmol) was added, and the reaction mixture was stirred at 30–32 °C for 1 h. After that, chloranil (185 mg, 0.75 mmol) was immediately added and the stirring continued for another 5 min at the same temperature. The reaction mixture was cooled to room temperature, hydrolyzed with 10% aq NaOH (18 mL), washed with water and brine, and dried over  $Na_2SO_4$ . The desiccant was filtered off, the solvent removed in vacuo and the residue separated by column chromatography (silica gel, 15 g, DCM) to give porphyrin 4a (27.4 mg, 16% yield) along with tetraphenylporphyrin 4b (14.6 mg, 10%). Porphyrin 4a: violet crystals;  $^1H$  NMR ( $CDCl_3$ , 300 MHz)  $\delta$  −2.72 broad s (2H), 6.98 s (2H), 7.6–7.9 m (11H), 8.2–8.35 m (6H), 8.37 pseudo d (2H,  $J = 8.28$  Hz), 8.8–9.1 m (8H);  $^{13}C$  NMR ( $CDCl_3$ , 75 MHz)  $\delta$  118.7, 120.3, 120.4, 124.0, 126.7, 127.8, 131.3 (broad m), 134.4, 134.6, 135.0, 141.8, 142.3, 169.6; IR (KBr,  $cm^{-1}$ )  $\nu$  3318 (NH), 1716 (C=O); HRMS-ESI calcd for  $C_{48}H_{32}N_4O_2^+ [M + H]^+$ , 710.2551, found 710.2538.

**Compound 12.** *Procedure A.* A mixture of aziridine 10 (59 mg, 0.2 mmol) and imide 11 (48 mg, 0.23 mmol) in dry chlorobenzene (5 mL) was heated under reflux for 32 h until all of the starting aziridine was consumed. After removal of the solvent under reduced pressure, the crude product was purified by column chromatography (petroleum ether/ethyl acetate 5:1) to give compound 13 as yellowish crystals (65 mg, 65% yield).

*Procedure B.* A mixture of aziridine 10 (74 mg, 0.25 mmol) and imide 11 (57 mg, 0.27 mmol) in dry chlorobenzene (3 mL) was subjected to microwave irradiation (160 W, maximum temperature achieved: 125 °C) for 45 min until all of the starting aziridine was consumed. Purification by column chromatography (petroleum ether/

ethyl acetate 5:1) gave compound 12 (119 mg, 95% yield): yellowish crystals; mp 124–126 °C;  $^1H$  NMR ( $CDCl_3$ , 300 MHz)  $\delta$  1.14 t (3H,  $J = 7.2$  Hz), 1.24 t (3H,  $J = 7.2$  Hz), 3.66 dd (1H,  $J_1 = 8.5$  Hz,  $J_2 = 1.0$  Hz), 3.75 s (3H), 4.01 dd (1H,  $J_1 = 9.7$  Hz,  $J_2 = 8.7$  Hz), 4.11 q (2H,  $J = 7.0$  Hz), 4.19 q (2H,  $J = 7.2$  Hz), 4.93 d (1H,  $J = 9.7$  Hz), 5.11 d (1H,  $J = 1.0$  Hz), 6.76 d (2H,  $J = 9.3$  Hz), 6.82 d (2H,  $J = 9.3$  Hz), 7.28 d (2H,  $J = 8.7$  Hz), 7.45 d (2H,  $J = 8.7$  Hz);  $^{13}C$  NMR ( $CDCl_3$ , 75 MHz)  $\delta$  13.9, 14.1, 46.9, 48.6, 55.4, 61.5, 62.0, 64.3, 65.4, 114.6, 118.1, 127.8, 129.4, 129.9, 134.8, 137.9, 154.4, 169.9, 170.8, 174.3, 174.5; IR (KBr,  $cm^{-1}$ )  $\nu$  1707 (C=O), 1734 (C=O), 1754 (C=O); HRMS-ESI calcd for  $C_{25}H_{26}ClN_2O_7^+ [M + H]^+$  501.1423, found 501.1416; calcd for  $C_{25}H_{25}ClN_2O_7K^+ [M + K]^+$  539.0982, found 539.0990.

**Compound 13.** *Procedure A.* A mixture of compound 12 (41 mg, 0.08 mmol) and  $MnO_2$  (178 mg, 2.05 mmol) in chlorobenzene (3 mL) was heated under reflux for 32 h. On completion of the reaction the oxidant was filtered off, the solvent removed in vacuo, and the product purified by column chromatography on silica gel (petroleum ether–ethyl acetate 5:1) to give pyrrole 13 as colorless crystals (14 mg, 35%).

*Procedure B.* A mixture of compound 12 (50 mg, 0.1 mmol) and DDQ (23 mg, 0.1 mmol) in chlorobenzene (3 mL) was subjected to microwave irradiation (160 W, maximum temperature achieved: 130 °C) for 45 min. On completion of the reaction the solvent was removed in vacuo and the product was purified by column chromatography on silica gel (petroleum ether–ethyl acetate 5:1) giving pyrrole 13 (48 mg, 97%): colorless crystals; mp 238–239 °C;  $^1H$  NMR ( $CDCl_3$ , 300 MHz)  $\delta$  1.32 t (6H,  $J = 7.1$  Hz), 3.89 s (3H), 4.28 q (4H,  $J = 7.1$  Hz), 7.02 d (2H,  $J = 8.7$  Hz), 7.24 d (2H,  $J = 8.7$  Hz), 7.37 d (2H,  $J = 8.7$  Hz), 7.48 d (2H,  $J = 8.3$  Hz);  $^{13}C$  NMR ( $CDCl_3$ , 75 MHz)  $\delta$  13.9, 55.4, 62.1, 113.8, 123.8, 124.4, 128.2, 128.3, 129.2, 129.8, 130.7, 133.8, 158.2, 160.3, 160.5; IR (KBr,  $cm^{-1}$ )  $\nu$  1778 (C=O), 1737 (C=O), 1719 (C=O); HRMS-ESI calcd for  $C_{25}H_{22}ClN_2O_7^+ [M + H]^+$  497.1110, found 497.1112; calcd for  $C_{25}H_{21}ClN_2O_7Na^+ [M + Na]^+$  519.0929, found 519.0952; calcd for  $C_{25}H_{21}ClN_2O_7K^+ [M + K]^+$  535.0669, found 535.0687.

**Porphyrin 4c.** A mixture of aziridine 10 (21 mg, 0.07 mmol, 1 equiv) and porphyrin 4a (49 mg, 0.07 mmol, 1 equiv) in dry chlorobenzene (5 mL) was subjected to microwave irradiation (160 W, maximum temperature achieved during the reaction: 126 °C) for 60 min. An additional portion of aziridine 10 (9 mg, 0.03 mmol, 0.3 equiv) was added, and irradiation was repeated for another 30 min. DDQ (35 + 10 + 5 mg, 0.22 mmol, 3 equiv) was added in three portions as denoted in parentheses followed by microwave irradiation under the same conditions for 1 h after each portion. Column chromatography (silica gel, petroleum ether/EtOAc) gave porphyrin 4c (32 mg, 46% yield): violet crystals;  $^1H$  NMR ( $CDCl_3$ , 300 MHz)  $\delta$  −2.74 broad s (2H), 1.43 t (6H,  $J = 7.1$  Hz), 3.91 s (3H), 4.38 q (4H,  $J = 7.1$  Hz), 7.06 pseudo d (2H,  $J = 8.7$  Hz), 7.32 pseudo d (2H,  $J = 8.7$  Hz), 7.7–7.8 m (9H), 7.86 pseudo d (2H,  $J = 8.2$  Hz), 8.20–8.35 m (6H), 8.39 pseudo d (2H,  $J = 8.2$  Hz), 8.75–8.95 m (4H), 8.91 pseudo d (2H,  $J = 5$  Hz), 8.98 pseudo d (2H,  $J = 5$  Hz);  $^{13}C$  NMR ( $CDCl_3$ , 75 MHz)  $\delta$  14.0, 55.5, 62.2, 113.9, 118.9, 120.2, 120.3, 124.1, 124.5, 125.2, 126.7, 127.7, 128.3, 129.9, 131.2, 132.0, 134.6, 135.1, 141.9, 142.1, 158.0, 160.4, 161.1; IR (KBr,  $cm^{-1}$ )  $\nu$  3313 (NH), 1731 (C=O); HRMS-ESI calcd for  $C_{63}H_{45}N_6O_7^+ [M + H]^+$  999.3501, found 999.3488.

**Porphyrinofullerene 5.** A mixture of aziridine 14 (15 mg, 0.013 mmol, 1 equiv) and porphyrin 4a (91 mg, 0.128 mmol, 10 equiv) in

dry chlorobenzene (10 mL) was heated at 90 °C for 21 h. The solvent was evaporated in vacuo, and unreacted porphyrin **4a** was removed by column chromatography (silica gel, 10 g, DCM/EtOAc, gradient from pure DCM to ratio 10:1). Using this procedure, a recovery of 89.5 mg of porphyrin **4a** was made and 19 mg of a crude mixture of cycloadducts **15** was achieved. Cycloadducts **15** thus obtained were dissolved in chlorobenzene (5 mL), DDQ (5 mg, 0.022 mmol, 2.2 equiv) was added and the reaction mixture was subjected to microwave irradiation (160 W, maximum temperature achieved during the reaction: 126 °C) for 30 min. Column chromatography (silica gel, 10 g, DCM/EtOAc, gradient from pure DCM to 10:1 ratio) gave porphyrinofullerene **5** (10 mg, 42% yield): purple-brown solid; <sup>1</sup>H NMR (CDCl<sub>3</sub>, 300 MHz) δ -2.82 broad s (2H, NH), 1.20 t (6H, J = 7.1 Hz, CH<sub>3</sub>), 1.40 t (6H, J = 7.2 Hz, CH<sub>3</sub>), 4.34 q (4H, J = 7.4 Hz, CH<sub>2</sub>), 4.40 q (4H, J = 6.8 Hz, CH<sub>2</sub>), 6.59 s (2H, CHCO<sub>2</sub>Et), 7.43 pseudo d (2H, J = 8.5 Hz, H<sup>arom</sup>), 7.52 pseudo d (2H, J = 8.4 Hz, H<sup>arom</sup>), 7.70–7.80 m (9H, H<sup>m+p(Ph)</sup>), 7.88 pseudo d (2H, J = 7.5 Hz, H<sup>arom</sup>), 8.20–8.30 m (6H, H<sup>(Ph)</sup>), 8.41 pseudo d (2H, J = 8.1 Hz, H<sup>arom</sup>), 8.85–9.05 m (8H, H<sup>pyrr</sup>); <sup>13</sup>C NMR (CDCl<sub>3</sub>, 125 MHz) δ 169.9 (C=O), 161.1 (C=O), 157.9, 153.1, 150.2, 147.5, 147.0, 146.4, 146.26, 146.25, 146.13, 146.12, 145.63, 145.5, 145.42, 145.35, 145.3, 144.43, 144.41, 143.1, 143.0, 142.8, 142.7, 142.38, 142.35, 142.17, 142.16, 142.1, 141.9, 141.8, 141.73, 141.68, 140.2, 139.6, 136.8, 136.0, 135.1, 134.7, 132.4, 131.5, 131.3 (broad s), 128.7, 127.8, 126.8, 125.4, 124.9, 124.3, 120.5, 120.4, 119.2, 118.7 (C<sup>arom</sup>), 74.9 (CH<sup>pyrr</sup>), 71.2 (C<sup>q<sub>pyrr</sub></sup>), 62.32 (CH<sub>2</sub>O), 62.30 (CH<sub>2</sub>O), 14.5 (CH<sub>3</sub>), 14.4 (CH<sub>3</sub>); IR (KBr, cm<sup>-1</sup>) ν 3314 (NH), 1732 (C=O); HRMS calcd for C<sub>130</sub>H<sub>56</sub>N<sub>7</sub>O<sub>10</sub><sup>+</sup> [M + H]<sup>+</sup>, 1874.4083, found 1874.4064; MS-FD calcd for C<sub>130</sub>H<sub>55</sub>N<sub>7</sub>O<sub>10</sub><sup>+</sup> [M]<sup>+</sup> 1874.4, found 1874.5.

## ■ ASSOCIATED CONTENT

### ● Supporting Information

<sup>1</sup>H and <sup>13</sup>C NMR spectra for all new compounds, the 2D-<sup>1</sup>H-COSY spectrum for compound **5**, CVA's at various rates for C<sub>60</sub>, ferrocene and compounds **3a–e**, **4a–c**, and **5**. Computational details: energies of molecules **2**, **3a–d**, and **4a–c** and their Cartesian coordinates of atoms. This material is available free of charge via the Internet at <http://pubs.acs.org>.

## ■ AUTHOR INFORMATION

### Corresponding Author

\*E-mail: [alexander.khlebnikov@pobox.spbu.ru](mailto:alexander.khlebnikov@pobox.spbu.ru).

### Notes

The authors declare no competing financial interest.

## ■ ACKNOWLEDGMENTS

We gratefully acknowledge the financial support of the Russian Foundation for Basic Research (Grant No. 11-03-00186) and Saint Petersburg State University (Grant No. 12.38.78.2012). This research used resources of the resource center “Computer Center” and “Center for Chemical Analysis and Material Research” of Saint Petersburg State University.

## ■ REFERENCES

- (1) Imahori, H.; Mori, Y.; Matano, Y. *J. Photochem. Photobiol. C: Photochem. Rev.* **2003**, *4*, 51.
- (2) Konishi, T.; Ikeda, A.; Shinkai, S. *Tetrahedron* **2005**, *61*, 4881.
- (3) Marcus, R. A.; Sutin, N. *Biochim. Biophys. Acta* **1985**, *811*, 265.
- (4) Imahori, H. *Org. Biomol. Chem.* **2004**, *2*, 1425.
- (5) Imahori, H.; Sakata, Y. *Eur. J. Org. Chem.* **1999**, 2445.
- (6) Ito, O.; D'Souza, F. *Molecules* **2012**, *17*, 5816.
- (7) D'Souza, F.; Ito, O. *Chem. Commun.* **2009**, 4913.
- (8) El-Khouly, M. E.; Ito, O.; Smith, P. M.; D'Souza, F. *J. Photochem. Photobiol. C: Photochem. Rev.* **2004**, *5*, 79.
- (9) Wessendorf, F.; Grimm, B.; Guldi, D. M.; Hirsch, A. *J. Am. Chem. Soc.* **2010**, *132*, 10786.

- (10) Araki, Y.; Ito, O. *Photochem. Photobiol. C: Photochem. Rev.* **2008**, *9*, 93.
- (11) MacMahon, S.; Fong, R.; Baran, P. S.; Safonov, I.; Wilson, S. R.; Schuster, D. I. *J. Org. Chem.* **2001**, *66*, 5449.
- (12) Schuster, D. I.; MacMahon, S.; Guldi, D. M.; Echegoeyn, L.; Braslavsky, S. E. *Tetrahedron* **2006**, *62*, 1928.
- (13) Schlundt, S.; Kuzmanich, G.; Spänig, F.; deMiguel Rojas, G.; Kovacs, C.; Garcia-Garibay, M. A.; Guldi, D. M.; Hirsch, A. *Chem.—Eur. J.* **2009**, *15*, 12223.
- (14) Kovacs, C.; Hirsch, A. *Eur. J. Org. Chem.* **2006**, 3348.
- (15) Yamada, H.; Ohkubo, K.; Kuzuhara, D.; Takahashi, T.; Sandanayaka, A. S. D.; Okujima, T.; Ohara, K.; Ito, O.; Uno, H.; Ono, N.; Fukuzumi, S. *J. Phys. Chem. B* **2010**, *114*, 14717.
- (16) Shibano, Y.; Sasaki, M.; Tsuji, H.; Araki, Y.; Ito, O.; Tamao, K. *J. Organomet. Chem.* **2007**, *692*, 356.
- (17) Fukuzumi, S.; Imahori, H.; Yamada, H.; El-Khouly, M. E.; Fujitsuka, M.; Ito, O.; Guldi, D. M. *J. Am. Chem. Soc.* **2001**, *123*, 2571.
- (18) Imahori, H.; Yamada, K.; Hasegawa, M.; Taniguchi, S.; Okada, T.; Sakata, Y. *Angew. Chem., Int. Ed. Engl.* **1997**, *36*, 2626.
- (19) Konev, A. S.; Khlebnikov, A. F.; Frauendorf, H. *J. Org. Chem.* **2011**, *76*, 6218.
- (20) Manna, T.; Bhattacharya, S. J. *Theor. Comp. Chem.* **2008**, *7*, 1055.
- (21) Williams, R. M. *Introduction to Electron Transfer*, e-book adapted from Fullerenes as Electron Accepting Components in Supramolecular and Covalently Linked Electron Transfer Systems, Ph.D. Thesis, Amsterdam, 1996.
- (22) Brédas, J. L.; Silbey, R.; Boudreaux, D. S.; Chance, R. R. *J. Am. Chem. Soc.* **1983**, *105*, 6555. Though correlations between IP and EA are described in the refs 22–26, these values are related to HOMO/LUMO energies via Koopmans' theorem.
- (23) Miller, L. L.; Nordblom, G. D.; Mayeda, E. A. *J. Org. Chem.* **1972**, *37*, 916.
- (24) Parker, V. D. *J. Am. Chem. Soc.* **1974**, *96*, 5656.
- (25) Loutfy, R. O.; Still, I. W. J.; Thompson, M.; Leong, T. S. *Can. J. Chem.* **1979**, *57*, 638.
- (26) Lee, Y.-Z.; Chen, X.; Chen, S.-A.; Wei, P.-K.; Fann, W.-S. *J. Am. Chem. Soc.* **2001**, *123*, 2296.
- (27) Mi, D.; Kim, H.-U.; Kim, J.-H.; Xu, F.; Jin, S.-H.; Hwang, D.-H. *Synth. Met.* **2012**, *162*, 483.
- (28) Konev, A. S.; Mitichkina, A. A.; Khlebnikov, A. F.; Frauendorf, H. *Russ. Chem. Bull., Int. Ed.* **2012**, *61*, 860.
- (29) Geometry optimizations of the molecules in the gas phase and using the PCM solvent model for 1,2-dichlorobenzene were performed at the B3LYP/6-31G(d) level. The optimized geometries were used for single-point RHF calculations of FMO energies in the gas phase and in 1,2-dichlorobenzene (see the Supporting Information). The experimental reduction and oxidation potentials were correlated with calculated FMO energies. The best correlation was found for the B3LYP/6-31G(d) FMO energies calculated in the gas phase, with R<sup>2</sup> having a value of 0.99. This correlation was used for further evaluations.
- (30) Boëns, B.; Faugeras, P. A.; Vergnaud, J.; Lucas, R.; Teste, K.; Zerrouki, R. *Tetrahedron* **2010**, *66*, 1994.
- (31) Manecke, G.; Klawitter, J. *Makromol. Chem.* **1971**, *142*, 253.
- (32) Sharghi, H.; Nejad, A. H. *Tetrahedron* **2004**, *60*, 1863.
- (33) Geier, G. R.; Lindsey, J. S. *Tetrahedron* **2004**, *60*, 11435.
- (34) Sharghi, H.; Nejad, A. H. *Helv. Chim. Acta* **2003**, *86*, 408.
- (35) Adler, A. D. *J. Org. Chem.* **1967**, *32*, 476.
- (36) Mirjalili, B. B. F.; Bamoniri, A.; Vafazadeh, R.; Zamani, L. *Bull. Korean Chem. Soc.* **2009**, *30*, 2440.
- (37) Nia, Sh.; Gong, X.; Drain, Ch. M.; Jurow, M.; Rizvia, W.; Qureshy, M. *J. Porphyrins Phthalocyanines* **2010**, *14*, 621.
- (38) Rahmatpour, A. *React. Funct. Polym.* **2011**, *71*, 80.
- (39) Mikus, A.; Bielińska, M. E.; Lipińska, T.; Ostrowski, S. *Synth. Commun.* **2011**, *41*, 3703.
- (40) Ló, S. M. S.; Ducatti, D. R. B.; Duarte, M. E. R.; Barreira, S. M. W.; Nosedá, M. D.; Gonçalves, A. G. *Tetrahedron Lett.* **2011**, *52*, 1441.
- (41) Caddick, S.; Fitzmaurice, R. *Tetrahedron* **2009**, *65*, 3325.

- (42) Kappe, C. O. *Angew. Chem., Int. Ed.* **2004**, 43, 6250.
- (43) Pineiro, M.; Pinho e Melo, T. M. V. D. *Eur. J. Org. Chem.* **2009**, 5287.
- (44) Appukkuttan, P.; Mehta, V. P.; Van der Eyken, E. V. *Chem. Soc. Rev.* **2010**, 39, 1467.
- (45) Kuznetsov, M. A.; Ushkov, A. V.; Selivanov, S. I.; Pan'kova, A. S.; Linden, A. *Russ. J. Org. Chem.* **2009**, 45, 1200.
- (46) Jiu, T.; Li, Y.; Gan, H.; Li, Y.; Liu, H.; Wang, H.; Zhou, W.; Wang, C.; Li, X.; Li, X.; Zhu, D. *Tetrahedron* **2007**, 63, 232.
- (47) Boscencu, R.; Oliveira, A. S.; Ferreira, D. P.; Ferreira, L. F. V. *Int. J. Mol. Sci.* **2012**, 13, 8112.
- (48) Gouterman, M.; Khalil, G. E. *J. Mol. Spectrosc.* **1974**, 53, 88. (The EPA mixed solvent (ethyl ether/isopentane/ethanol in volume ratio of 5:5:2.)
- (49) Stasio, B. D.; Frochot, C.; Dumas, D.; Even, P.; Zwier, J.; Guillemin, F.; Viriot, M. L.; Barberi-Heyob, M. *Eur. J. Med. Chem.* **2005**, 40, 1111.
- (50) Demas, J. N.; Crosby, G. A. *J. Phys. Chem.* **1971**, 75, 991.
- (51) Seybold, P. G.; Gouterman, M. *J. Mol. Spectrosc.* **1969**, 31, 1.
- (52) <http://www.obbcorp.com/systems/bench-top-fluorometers/EasyLifeX/EasyLife-X-Data.html>, accessed February 19, 2013.
- (53) Gupta, I. T. I.; Ravikanth, M. *J. Chem. Sci.* **2005**, 117, 161.